Current Applied Physics 10 (2010) 1123–1131

Contents lists available at ScienceDirect

Current Applied Physics

journal homepage: www.elsevier.com/locate/cap

Cathodoluminescence studies of un-doped and (Cu, Fe, and Co)-doped tin dioxide films deposited by spray pyrolysis

G. Korotcenkov [a,*], B.K. Cho [b,*], M. Nazarov [a], Do Young Noh [a], E.V. Kolesnikova [c]

[a] Department of Material Science and Engineering, Gwangju Institute of Science and Technology, Republic of Korea
[b] Department of Nanobio Materials and Electronics, and Department of Materials Science and Engineering, Gwangju Institute of Science and Technology, Republic of Korea
[c] Ioffe Physico-Technical Institute, Russian Academy of Sciences, St. Petersburg, Russia

ARTICLE INFO

Article history:
Received 21 September 2009
Received in revised form 13 January 2010
Accepted 25 January 2010
Available online 2 February 2010

Keywords:
Metal oxides
Thin films
Deposition
Doping
Cathodoluminescence

ABSTRACT

Un-doped and (Cu, Fe, and Co)-doped SnO_2 were studied using films deposited by spray pyrolysis. Room temperature cathodoluminescence (CL) was measured. Differences in CL spectra were observed as a function of deposition parameters (T_{sub}-350–550 °C), the nature and concentration of dopants (0–16 at.%), and the resulting high annealing temperature (T_{an} = 700–950 °C). A possible luminescence mechanism has been discussed. It was established that changes taking place in CL spectra were caused by the change of both the grain size and crystallinity (stoichiometry) of the surface layer. It was concluded that radiative recombination occurs through shallow donor levels associated with O-vacancies and trapped centers. It was assumed that in SnO_2 there are apparently three types of defects forming deep levels located at 0.8–0.9, 1.3–1.4, and ~1.6 eV from the top of the valence band.

1. Introduction

Numerous studies have shown that gas sensing properties of metal oxides have a strong dependence on their structural properties, such as the type and the concentration of point defects, which can be generated in metal oxide during synthesis and interaction with the surrounding atmosphere [1–3]. Therefore, the study of both the mechanism of structural defects' formation in the metal oxides and regularities of their influence on metal oxides properties has special meaning. In many cases, this type of data has been obtained during analysis of electrophysical properties [4,5]. However, such analysis has considerable limitations, and requires a wide range of measured temperatures. Also, it does not always provide complete information about both the nature of those centers, or their energy position in a semiconductor's band gap. Therefore, it is necessary to extend research methods, used for obtaining additional information about structural properties of metal oxides and their associated energy-level systems, as presented in band gap, so as to extend our knowledge about these defects, either extant or generated in a semiconductor as a result of various effects.

In this context, using cathodoluminescence measurements as an additional method of a metal oxide's characterization is very promising. As used here, cathodoluminescence (CL) is understood to be the emission of light from a material under electron bombardment. From the change of intensity of emitted cathodoluminescence, one can receive additional information about the lattice disordering in studied material.

In recent years, CL has been used intensively for the study of the properties of various metal oxides, including both SnO_2 one-dimensional structures and un-doped SnO_2 powders [6–14]. However, the investigation of luminescence properties of thin films, especially doped SnO_2 films, remains very limited. Only a few such studies were concerned with doped SnO_2 films [6,15–18]. As is generally known, the luminescence in polycrystalline and nanocrystalline metal oxides is usually weaker and lacks the fine structure of emission spectra characteristic for the bulk crystals. Nevertheless, a study of the luminescence spectra of the SnO_2 thin film is interesting and important because this material has great advantages for large-scale applications in various devices, such as solar cells, gas sensors, thin film field transistors and magnetic memory [19–22]. Besides, the cathodoluminescence study can provide valuable information on the quality and purity of these materials.

In the work, reported here, we have continued researching (Co, Cu, and Fe)-doped SnO_2 films started before. The analysis of the cathodoluminescence properties of the above-mentioned films was carried out with aims to clarify (i) how the deposition parameters and concentration of dopants influence the cathodoluminescence of SnO_2, (ii) what transformations in the CL spectra take place during high temperature annealing, as well as (iii) what the

* Corresponding authors. Address: Department of Material Science and Engineering, Gwangju Institute of Science and Technology, 261 Chemdan-gwagiro, Buk-gu, Gwangju 500-712, Republic of Korea. Tel.: +82 62 970 2354; fax: +82 62 970 2304.
E-mail addresses: ghkoro@yahoo.com (G. Korotcenkov), chobk@gist.ac.kr (B.K. Cho).

1567-1739/$ - see front matter © 2010 Elsevier B.V. All rights reserved.
doi:10.1016/j.cap.2010.01.012

correlation is between the film structure and the CL spectra? Concerning the results of a previous study, carried out on present samples, they are presented in Refs. [19,23–25]. In particular the Ref. [25] is dedicated to detailed structural characterizations of undoped SnO_2 films. The results, connected with analysis of the doping influence on the film structure and its thermal stability, are discussed in Refs. [23,24]; while the results, relative to gas sensing properties of those films, can be found in Refs. [19,23].

2. Experimental details

For the experiments discussed herein, we have used SnO_2 samples similar to the ones described in [23–25]. SnO_2 films, doped by Fe, Cu, and Co were deposited onto a single-crystal Si substrate using a spray pyrolysis method from 0.2 M $SnCl_4$–water solution [26,27]. The substrate temperature (T_{sub}) during film deposition was varied in the range from 350 to 550 °C. Our experiments showed that this temperature range is optimal for deposition of SnO_2 films aimed for gas sensor applications [26,27]. Dopants were embedded into solution in the form of chlorides. The concentration of doping elements in sprayed solution was varied from 0 to 16 at.%. The concentration of those elements in deposited films was smaller than in sprayed solution. However, this difference was not great. For example, while the concentration of the doping elements in the sprayed solution equaled 16 at.%, the concentration of Co, Cu, and Fe in the SnO_2 films with thickness ~250 nm (T_{sub} = 450 °C), estimated by using an EDX method, was 10–15, 10–12, and 10–13 at.%, respectively. The thickness of films studied varied from 40 nm to 400 nm. In particular, we analyzed CL spectra of the films with thickness 40–50 nm, 50–60 nm, 90–100 nm, 120–150 nm, ~250 nm and ~400 nm. The wide range of the thicknesses was a consequence of the fact that SnO_2 films find applications in devices that require a very wide range of thicknesses.

Room temperature CL measurements were conducted, using a spectrometer, recording radiation in the range 300–850 nm [28]. The CL spectra were excited in vacuum in the camera of a standard micro-probe analyzer Camebax-4. The samples were irradiated by an electron beam with a diameter up to 1 μm. The luminescence emitted was collected through the quartz window of the unit's camera. The data acquisition and processing system contained a photo-electric multiplier (ФЭУ-106). Radiation was detected in the photon-counting mode. The obtained spectra have not been corrected for the optical response of the measurement system. During our experiments, we took special care in collecting spectra in order to have comparable results in CL intensity, which is fundamental to this paper. Thus, for this reason, the parameters of the experiment such as the configuration of measurement system, excitation energy, diameter of the electron beam, and the electron current were the same during all of our experiments. In addition, the obtained results were averaged for several measurements at different points.

The conditions of excitation were selected in order to insure that at maximum intensity of CL the electron beam did not interact with substrate. In particular, for samples studied by us, optimal conditions of measurement have been observed at excitation energies 10–15 kV, and electron currents from 30 to 100 nA. According to our estimations at the indicated conditions, the depth of cathodoluminescence generation changed from 500 nm to 1 μm. That meant that for our films the substrate could have an influence on recorded CL spectra. However, it is necessary to note that the Si substrate does not have any luminescence in tested spectral range and the thickness of native oxide (SiO_2) present on the surface of Si substrate is very small. A laser ellipsometer measurement showed that the thickness of SiO_2 layer was smaller than 3 nm. Thus, on the basis of the above-mentioned conditions, the influence of the substrate on measured CL spectra can be neglected. Follow-up measurements confirmed our assertion. Obtained spectra were strongly dependent on parameters of deposited SnO_2 films. Moreover, we did not observed in CL spectra any bands characteristic for silicon dioxide [28], the intensity of which was being increased as the SnO_2 film thickness decreased. A good correlation of recorded CL spectra with spectra of SnO_2 powders and nanowires, where we do not have any influence on the substrates, is another confirmation of the above mentioned statement. Optical transmission spectra of SnO_2 films deposited on quartz substrates were measured in the near UV spectral range by an SDL-1 spectrometer using a 100 W halogen lamp.

Thermal treatments of SnO_2 films were carried out in temperature range 700–950 °C in the atmosphere of air during 1 h. As it was shown earlier, the annealing at lower temperatures exerts weak influence on the CL spectra of metal oxides [7,29].

3. Experimental results and discussion

3.1. Cathodoluminescence of un-doped SnO_2 films

Typical CL spectra of un-doped SnO_2 films with thicknesses larger than 100 nm are shown in Fig. 1. It is seen that deposited films have a broad peak of cathodoluminescence with maximum, centered at $\lambda \sim 500$ nm. CL spectra have a shape, typical for emission spectra, observed for SnO_2 powders, which also have broad peaks of either cathodoluminescence with a maximum, centered at $\lambda \sim 500$ nm [7,30]. Analogous shapes were also observed for spectra of radiative recombination, measured for SnO_2 quasi one-dimensional nanostructures such as nanowires, nanoribbons, [7,11]. Independent of deposition temperature broad peaks were centered in the spectral range from 510 to 570 nm. Some additional information about CL spectra of SnO_2 powders and nanowires is presented in Table 1. Some characteristic parameters of typical PL spectra of SnO_2 nanowires and powders are also presented for comparison in this table.

Cathodoluminescence emission in metal oxides generally takes place according to one of two mechanisms [12,36,37]. The first mechanism is a direct transition across the band gap. Due to SnO_2 at 300 K having E_g = 3.6 eV [8,15], the emission connected with these transitions must be observed in the spectral range 345–350 nm. The second mechanism is due to transitions between localized electronic states, introduced by lattice defects, such as interstitial defects, dangling bonds, vacancies, or impurities. It is known that oxygen vacancies in SnO_2 generate localized states in the form of shallow donor levels approximately 0.03–0.3 eV below the bottom of the SnO_2 conduction band. So, the emission related to the transitions with the participation of these shallow levels must be in the range 375–380 nm. It means that observed lumines-

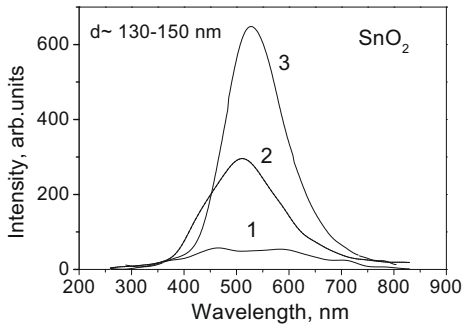

Fig. 1. Room temperature cathodoluminescence spectra of un-doped SnO_2 films deposited at (1) T_{sub} = 320 °C, (2) 450 °C, and (3) 550 °C; $d \sim$ 130–150 nm.

Table 1
Cathodoluminescence peaks generally observed for un-doped SnO_2 at room temperature.

Type	T (°C)	d (nm)	Method	Peak position (nm)								Refs.
				Violet/blue		Yellow–green			Orange			
Nanowires	450	>50	CL			455		520	570[m]		635	[7]
Nanowires	700	>20	CL			450	512[m]					[7]
Nanobelts		30–50	CL			450			560[m]			[11]
Powders	1000		CL			470		520[m]	560		650	[7]
Powders	250	4–5	CL			480					640[m]	[30]
Powders	600	17	CL				500[m]				650	[30]
Powders	1200	>200	CL			480		540	560		639[m]	[31,32]
Nanoribbons	900	50–250	PL							597[m]	640	[33]
Nanoribbons	1080	30–150	PL	392	439[m]	486	496					[34]
Powders		7	PL					530[m]			670	[35]
Powders	1350		PL	420						590[m]		[9]

CL – cathodoluminescence; PL – photoluminescence; m – maximum intensity; d – diameter of nanowires or grain size; T – temperature of deposition, calcinations or synthesis.

cence bands cannot be ascribed to both the direct recombination of conduction electrons with holes in the valence band and transitions with participation of shallow acceptor and shallow donor levels.

On the basis of the analysis that was carried out, one can conclude that observed CL spectra of as-deposited SnO_2 films can be explained only in the frame of mechanism taking into account transitions through electronic states in the middle of the SnO_2 band gap. It means that SnO_2 films, as well as powders and nanowires synthesized at low temperatures, are far away from structural perfection, i.e. the exterior crystalline perfection, observed for nanowires. However, this is not a basis for concluding that one-dimensional structures are free from structural (point) defects. We have made the same conclusion earlier analyzing cathodoluminescence spectra of In_2O_3 films and nanowires [38]. Thus, it is necessary to note that this conclusion has a real basis, because the concentration of point defects in metal oxides should be mainly determined by the temperature of synthesis and partial pressure of oxygen, which do not differ strongly from each other during films deposition and nanowires synthesis. Considerable difference takes place only for rate of the growth, which is essentially lower during synthesis of one-dimensional structures than during film deposition, especially using spray pyrolysis technology.

Studies have shown also that the main result of the increase in the deposition temperature is the growth of CL intensity and some narrowing of the emission band (see Fig. 1). Main changes of FWHM (full width at half maximum) of observed CL spectra take place at deposition temperatures lower than 400 °C. Such behavior is in good compliance with crystallinity improvement of the films deposited at higher temperatures. It is known that the increase of the concentration of defects usually is accompanied by the broadening of CL and photoluminescence peaks. At $T_{sub} > 450$ °C, the FWHM of main emission bands practically does not change and equals approximately 150 nm. In addition, it has been established that the higher the temperature of the substrates during SnO_2 film deposition is, the smaller is the discrepancy of CL spectra during the changing of either sample or the area of testing. In other words, luminescent properties and structural properties of SnO_2 films, deposited at higher temperatures, are more reproducible.

With a decrease of the deposition temperature, some transformation of the spectra also takes place. In the spectra of SnO_2 films, deposited at low temperatures ($T_{sub} \sim 350$ °C), the emission band, peaked at $\lambda \sim 350$–400 nm. This band is observed in the range of band–band transitions. However, we believe that this emission band has another nature. According to our assumption, this band is connected with quantum size effects. It is known that the decrease of grain size smaller than 2–3 nm provides a blue shift of both the ultra violet absorption edge and luminescence peaks of SnO_2 [39,40]. As established in research shown in Refs. [23,24], the appearance of such grains in SnO_2 films deposited at low temperatures is real. The absence of the above-mentioned band in CL spectra of thick enough SnO_2 films ($d > 100$ nm) deposited at $T_{sub} > 450$ °C confirms this conclusion. Films deposited at those temperatures usually have grain size larger than 6–8 nm [25].

As a result of comparison of CL spectra for films having various thicknesses, we have established also that for films, deposited at $T_{sub} \sim 520$–550 °C, the thickness in the range 60–400 nm has a weak influence on the shape of the cathodoluminescence spectra. We observed only a decrease of CL intensity for films with smaller thicknesses. The indicated change is in full accordance with decrease of both the SnO_2 grain size and "sampling volume". However, for films deposited at temperature lower than 420 °C, that influence is much stronger. Already at a thickness smaller than 120 nm, a considerable decrease of the CL intensity takes place. For films deposited at higher temperatures the same strong decrease of CL intensity takes place only at film thickness smaller 50–60 nm. It is necessary to note that the above-mentioned difference corresponded to observed changes in SnO_2 film morphology. As it was established in previous paper [25], if SnO_2 films deposited at low pyrolysis temperature ($T_{sub} < 420$ °C) consist of small spherulite-type grains, SnO_2 films deposited at higher temperatures usually consist of larger crystallite-type grains with clearly shown faceting the size of which is increased when both the film thickness and deposition temperature are increased.

3.2. Doping influence on cathodoluminescence spectra

The typical influence of doping on CL spectra of SnO_2 films is shown in Fig. 2. If these spectra are compared with spectra of un-doped SnO_2 films, one concludes that the doping does not

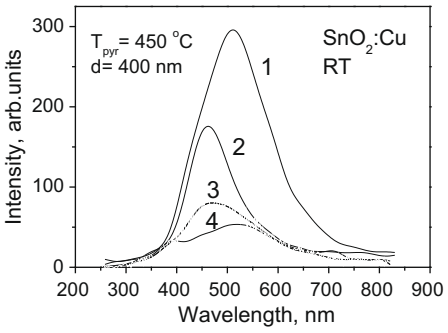

Fig. 2. CL spectra of SnO_2 films doped by Cu: $T_{sub} = 450$ °C; $d \sim 250$ nm; (1) un-doped SnO_2; (2) Cu 1 at.%; (3) Cu 4 at.%; and (4) Cu 16 at.%.

change the general picture of CL spectra of as-deposited SnO_2 films. At those spectra the same bands with some shifting in short-wavelength areas are dominant.

Such behavior of CL of doped SnO_2 is a known fact. For example, earlier this effect was observed for SnO_2 samples, doped by iron [6]. The authors observed for SnO_2–Fe (5%) the blue-shift of photoluminescence spectra equaled ~20 nm. They believed that this shift has been attributed to a higher strain and a reduced crystallite size in Fe-doped films.

At the same time, we established that the doping is accompanied by a sharp quenching of cathodoluminescence in comparison with un-doped samples. The strongest decrease of the cathodoluminescence intensity was observed for films deposited at high temperatures during doping by Cu and Fe (see Fig. 3). CL spectra of SnO_2 samples doped by Cu had the most clearly shown band in the range of ~350–400 nm as well (see Fig. 2). However, when doping with Co this influence was considerably smaller.

It is important that the regularities of the doping influence on the cathodoluminescence intensity of SnO_2 are in good accordance with the results of the doping influence on the structural properties of SnO_2 films. The results of last research were discussed in Refs. [23,24]. It was shown that the SnO_2 doping by Cu, Fe, and Co was accompanied by both the decrease of grain size and considerable increase of the contents of finely-dispersed amorphous-like phases with grain sizes smaller than 2–3 nm. Moreover, the higher the doping concentration was, the aforementioned effect was even stronger. According to the conception proposed in Ref. [23], the finely-dispersed phase is formed at the surface of SnO_2 crystallites and can fill inter-crystallite space. We assumed that the second oxide, due to the precipitation at the surface of SnO_2 grains, creates the additional nucleation centers for the SnO_2 growth, and, therefore, the growth of the SnO_2 film during deposition takes place not only due to the increase of the size of crystallites incipient at the primary stage of growth, but also due to the appearance of new grains, having a considerably smaller size in comparison with the already present crystallites appearing at the initial stages of the SnO_2 film's growth. As it was shown in Refs. [23,24], an especially strong influence on SnO_2 film structure takes place during doping by copper and iron. As is seen in Fig. 3, specifically for SnO_2 doped by Cu and Fe, we observe the maximum decrease of CL intensity.

However, the decrease of cathodoluminescence intensity takes place not in proportion to the increase of the contents of finely-dispersed amorphous-like phases, as noted in Ref. [23,24]. According to our estimations, the contents of finely-dispersed phases do not exceed 50%. Even more, as our research has shown [23,24], doped films even at the maximum concentration of dopants contain crystallites with sizes similar to the size of the crystallites in un-doped SnO_2 films. The average size of the crystallites in both un-doped and doped SnO_2 films (T_{sub} = 450 °C, $d \sim 120$ nm) estimated on the basis of X-ray diffraction (XRD) and scanning electron microscopy (SEM) measurements is equal to 25–30 nm. This demonstrates that the increase of the contents of the finely-dispersed amorphous-like phases is not the only reason for the observed quenching of the cathodoluminescence. Apparently, the deterioration of film crystallinity and the growth of the concentration of structural defects in doped films are more important reasons for the observed change of the CL spectra.

The coincidence of the CL emission intensities of heavily doped films, deposited at high temperatures, and SnO_2 films, deposited at low temperatures, which are structurally less perfect [41,42], directly confirms what was said before. As one can see from the results presented in Fig. 3, at the maximum concentration of dopants the intensity of cathodoluminescence drops down to the level, corresponding to CL intensity, measured for the samples, deposited at low temperatures (see Fig. 4 curve 4). It is important that for films deposited at low temperatures, the CL intensity is so low that dopants practically do not noticeably influence the CL spectra. Apparently, the concentration of structural defects is so high that the probability of non-radiative recombination of excitable electrons and holes appreciably exceeds the probability of radiative recombination.

The shape of CL spectra of heavily doped samples coincides with the shape of CL for films deposited at low temperatures as well (see Figs. 1 and 2). As it is seen from Fig. 2 in CL spectra of heavily doped samples, just as in the CL spectra of the films deposited at low temperatures (see Fig. 1), bands, peaking at the same wavelength 400 and 670 nm, start to become dominant. It indicates that the structure of the energy levels in these samples is similar.

The diffusion of the band gap edge showing the appearance of the tails of electronic states inside the SnO_2 band gap also indicates the increase of structural defects' concentration in heavily doped SnO_2 samples [19]. At that point the degree of the change in optical transmission near the band gap edge observed at SnO_2 doping (see

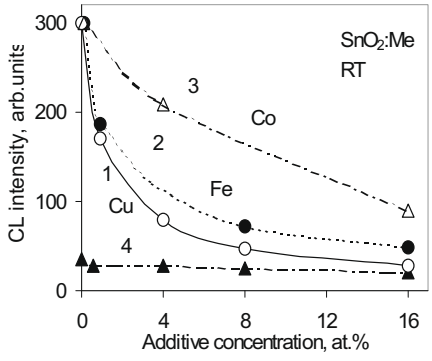

Fig. 3. Influence of (1) Cu, (2) Fe, and (3) Co concentration in a sprayed solution on the intensity of CL for SnO_2 films deposited at T_{sub} = 450 °C ($d \sim 120$ nm). Curve 4 corresponds to CL intensity of the films deposited at 350 °C.

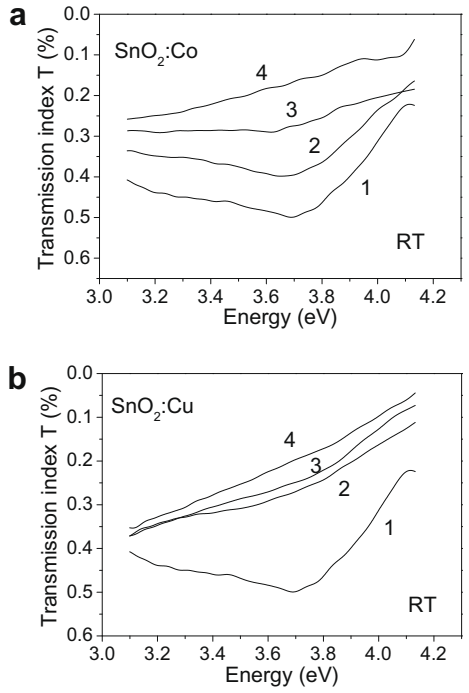

Fig. 4. Influence of doping by (a) Co and (b) Cu on transmission spectra of SnO_2 films deposited at T_{sub} = 450 °C: $d \sim 400$ nm; (1) un-doped; (2) 1 at.%; and (3) 4 at.%; (4) 16 at.%.

Fig. 4) is in good accordance with results presented earlier of the doping influence on the CL intensity.

If one can compare data presented in Fig. 4a and 4b for SnO_2:Cu and SnO_2:Co with results presented in Fig. 3, it is seen that the stronger diffusion of the band gap edge is, the larger the decrease of the CL intensity. The appearance near the SnO_2 valence band of the electronic states, introduced by lattice disordering caused by SnO_2 doping was also experimentally confirmed in Ref. [41]. Authors of [14] analyzed the results of an X-ray Photoemission Spectroscopy (XPS) study of SnO_2 powders after Ar-ion bombardment and doping by Pd and Pt.

3.3. Cathodoluminescence spectra transformation during thermal treatment

Cathodoluminescence spectra for both un-doped and doped SnO_2 films after various thermal treatments are shown in Figs. 5–8.

It is seen that high temperature annealing has great consequences for CL, which are as follows: (1) a sharp increase of CL intensity at $T_{an} > 800$ °C; and (2) a considerable transformation of spectra, especially in the range of 300–450 nm. Thus, we have two clearly shown regularities. The first regularity is characteristic for SnO_2 films with thicknesses larger than 200–300 nm deposited at $T_{sub} > 400$ °C. For such films, after annealing at $T_{an} > 850$ °C, we observed the appearance of the intensive short-wavelength band peaked at 375 nm close to the band-edge luminescence (see Figs. 7 and 8). For SnO_2 films with a thickness less than 200 nm, we did not observe the appearance of this band. For CL spectra the emission with a maximum, peak at $\lambda \sim 500$ nm continues to be dominant (see Fig. 6).

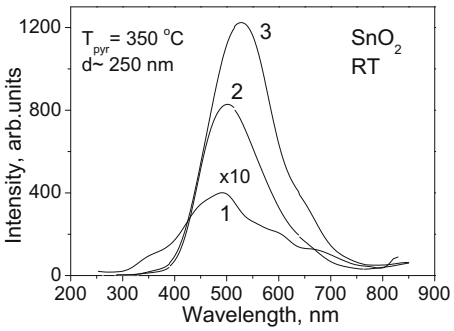

Fig. 5. CL spectra of un-doped SnO_2 films ($d \sim 250$ nm) deposited at $T_{sub} = 350$ °C after different thermal treatments: (1) as deposited; (2) $T_{an} = 850$ °C; and (3) $T_{an} = 950$ °C.

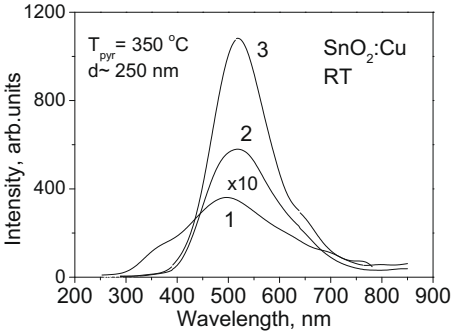

Fig. 6. CL spectra of Cu-doped (16 at.%) SnO_2 films ($d \sim 250$ nm) deposited at $T_{sub} = 350$ °C after different thermal treatments: (1) as deposited; (2) $T_{an} = 850$ °C; and (3) $T_{an} = 950$ °C.

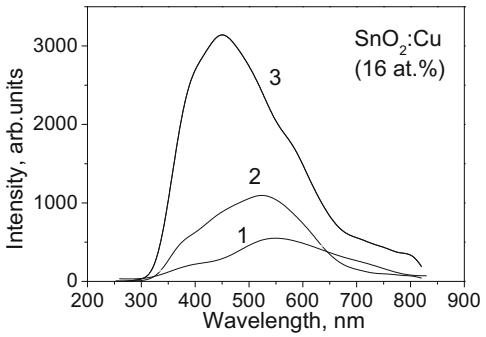

Fig. 7. CL spectra of Cu-doped (16 at.%) SnO_2 films deposited at $T_{sub} = 450$ °C: $d \sim 400$ nm; (1) as-deposited; (2) $T_{an} = 850$ °C; and (3) $T_{an} = 950$ °C.

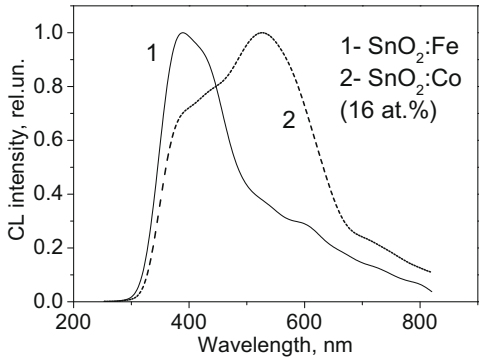

Fig. 8. Normalized CL spectra of (1) SnO_2:Fe and (2) SnO_2:Co films deposited at $T_{sub} = 450$ °C ($d \sim 400$ nm) after annealing at 950 °C.

The second regularity is characteristic for SnO_2 films deposited at low pyrolysis temperatures ($T_{sub} < 400$ °C). As we wrote earlier in part 3.1, in CL spectra of such films the band in the range of 350–400 nm is already shown (see Figs. 1 and 3). However, this band has a much smaller intensity and a larger FWHM than in first case. Moreover, after annealing at $T_{an} > 700$ °C, this band disappeared (see Figs. 5 and 6). It means that the nature of radiation peaks in the range of 350–400 nm observed in the CL spectra of SnO_2 films deposited at low temperatures and in the CL spectra of SnO_2 films subjected to high temperature annealing are different. As it was shown in Ref. [29], the annealing of the film first of all leads to coalescence of the smallest grains. Therefore, in films annealed at $T_{an} > 700$ °C, we do not have grains with sizes smaller than 3–5 nm, and therefore one can neglect quantum size effects which were used to explain the appearance of the 350–400 nm band in the CL spectra of SnO_2 films deposited at low temperatures. It means that observed position of CL peaks for annealed SnO_2 films corresponds to the real energy structure of defects which is responsible for radiation recombination.

It should be noted that the increase of quantum efficiency of luminescence after a high temperature annealing at 1000–1200 °C, which results in a considerable growth of crystallite size, is well-known fact [43,44], and it is widely used in the technology of phosphorus. The same growth of the CL intensity was observed during calcinations of SnO_2 powders [7], when the increase of annealing temperature was accompanied by the considerable growth of SnO_2 grain size. The observed similarities in the behavior of the CL properties in either powders or films during the annealing process reflects the similarity of the processes taking place in those materials.

Comparing the CL spectra of doped and un-doped SnO_2 films, one can conclude also that, in spite of the similar influence of the high temperature treatment on the CL intensity, the consequences

of the doping for the shape of CL spectra depend on the nature of the dopants used. As it is seen from Figs. 5–8, the correlation of the intensities of individual bands in the CL spectra of SnO_2 doped by various elements is different. For example, in the case of doping with iron, the CL spectra of the SnO_2 films with thicknesses ~400 nm the band peaked at 380 nm, while with doping using copper the band peaked at 450 nm with larger intensity. Doping with cobalt the band with the maximum intensity is peaked at 530 nm (see Figs. 7 and 8). It means that the dopants have their own specificity of interaction with the structural defects of SnO_2. Thus, due to preferable interactions with structural defects of certain types, the doping could appreciably change the concentration of point defects in comparison with un-doped materials.

So taking into account all of the obtained data, one can conclude that observed changes in CL spectra during thermal treatments are a consequence of the change of both the concentration of the structural defects, and the crystallite's size in the SnO_2 films namely, the decrease of the concentration of structural (point) defects and the increase of the grain size with the increase of the annealing temperatures. As is known, the growth of the grains during high temperature annealing is an inevitable process for all metal oxides that is independent of their initial state. This effect was observed experimentally for both films and powders [19,29].

It is quite possible that structural perfection and the grain size are to some extent interconnected. As we have mentioned before, we did not observe the appearance of a short-wavelength band centered at 370 nm for films with thicknesses smaller 200 nm (i.e. with the crystallite size smaller than 30–50 nm) even after thermal treatment at $T \sim 1000$ °C [23]. We need to note that during the study of CL spectra of SnO_2 powders with grain sizes between 27 and 29 nm that we also did not observe the appearance of short-wavelength peaks near the band-edge luminescence after thermal treatment at $T_{an} = 800$ °C [30]. In the work [7] where after calcination at $T_{an} = 800$ °C the crystallite size was ~47 nm, the short-wavelength peak at $\lambda < 400$ nm was not observed as well. As it follows from our experimental results, the short-wavelength band appears in CL spectra of SnO_2 after annealing at $T_{an} > 850$ °C only for thick films ($d > 200$ nm) in which, according to XRD and SEM measurements, the crystallite size could reach 80–100 nm [23–25]. It is a well-known fact that the grain size in films deposited on a heated substrate depends strongly on the film thickness [25,27].

We believe that the above-mentioned regularities are consequences of non-uniform distribution of structural defects inside of the SnO_2 grains. High resolution transmission electron microscopy (HRTEM) images of SnO_2 grains presented in Ref. [45] and the analysis of the results of Raman spectroscopy carried out in Ref. [46] show that in many cases, especially if the SnO_2 is synthesized at low temperatures or the SnO_2 grain size is smaller than 7 nm, the particles of SnO_2 consisted of a well-crystallized core covered with an amorphous layer of tin oxide. According to Ref. [46], the thickness of this layer has been calculated to be ~1.1 nm, (i.e. about two to three unit cells). It means that in grains (crystallites) with small size deposited at low temperatures, which were not subjected to an additional high temperature treatment, the role of the surface amorphous or structurally disturbed layer would be very strong in the forming of those grains' properties. Structural defects in that layer could be effective centers of non-radiative recombination blocking radiative recombination.

The results, published in Ref. [47] are another confirmation of the reliability of our assumptions. That study, in Ref. [47], has shown that in some nanomaterials, such as SnO_2, the grain boundary could be amorphous or crystalline, depending on the heat treatment and other processing conditions. In particular, according to Ref. [48], the SnO_2 grains with sizes between 2 and 5 nm have an amorphous grain boundary, whereas for grains with sizes between 5 and 10 nm, after annealing at 500 °C during 72 h, have a thin and crystalline grain boundary. At the same time, the conventional tin dioxide with a grain size larger than 100 nm does not have an amorphous grain boundary under any circumstances.

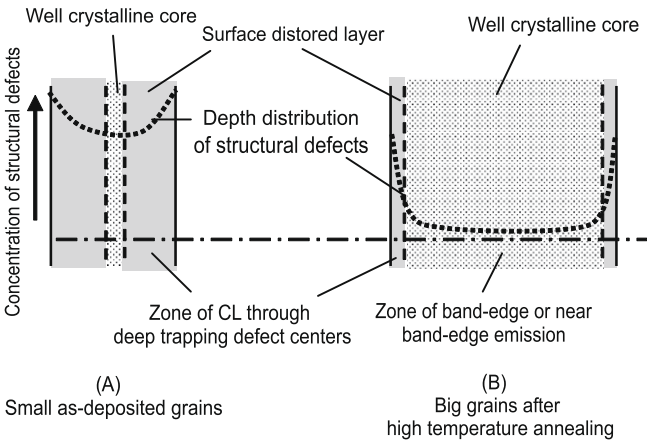

Fig. 9. Diagram illustrating the structure of SnO_2 grains.

Thus, it becomes clear that because of a considerable difference in distribution of the concentration of structural defects within grains that the SnO_2 grains (crystallites) may have areas with fundamentally different luminescence properties. For example, in a well-crystallized core the radiative recombination of electrons and holes through shallow donor and acceptor levels could predominate. In the surface area where the concentration of structural defects is high, the recombination of electrons and holes may have non-radiative nature, or may take place with the participation of deep-trapping centers in the SnO_2 band gap. A diagram illustrating this model is shown in Fig. 9.

Therefore, depending on the correlation between a well-crystallized core and disordered surface layer, the intensity and the shape of the CL spectra of SnO_2 would differ from each other greatly. The presence of a space charge region in the grain with a thickness comparable to the grain size, due to space separation of excitable electrons and holes, would promote the increase of the role of the surface structural disordered area in the CL spectra forming. As is known for SnO_2 being in an oxygen containing atmosphere, the band bending could reach 1.0 eV [19]. At the same time the increase of the deposition temperatures and the temperature of the following annealing, due to such effects as the ordering of the surface layer structure, the decrease of the structural defects' concentration, and the increase of the grain size, would all promote the strengthening of the role of a well-crystallized core in the CL spectra forming. The increase of the film thickness due to influence on grain size also should provide the same effect. As one can see from results presented earlier, those very regularities have been observed in our experiments.

The approach that we suggest for explaining the observed dependencies completely coincides with the results, obtained in Ref. [10] for ZnO synthesized for varistor applications. It was established that in the case of pure zinc oxide that the CL intensity at the grain boundary is lower than within the grain cores. Even more, the CL spectra in this area did not contain a short-wavelength band corresponding to band-edge luminescence. The short-wavelength peak was present only at the central area of the grain.

It is important that this model works for doped SnO_2 films as well because the doping, especially at a high concentration of additives (with the resultant decrease of grain size and the increase of structural disordering [23]), must promote an increase in the role of a highly defective surface area in forming the CL spectra. The authors of Ref. [41] established that the lattice distortion of SnO_2

grains conditioned by the presence of dopants is basically localized in the external layers of the nano-grains (i.e. in their surface area).

Substantial non-uniformity in the structural defects' distribution along the grain's depth [47] could also be a reason for the appearance in the grain of a considerable mechanical strain [48] which, according to the conclusions made in [10], also can promote the quenching of luminescence. The decrease of lattice distortion and the disappearance of mechanical strains in the bulk of the SnO_2 grains after annealing at the same temperatures (T_{an} > 500–700 °C) [48] when the transformation of the CL spectra begins and the growth of CL intensity [30] corresponds to our model conception.

3.4. Model of energy levels in the SnO_2 band gap

Analyzing the results, presented in Table 1 and in Figs. 1–8, one can conclude that the observed CL spectra are a superposition of 4–5 bands characterized by large broadening and mutual overlap. Thus, the fact that those peaks have different character dependencies upon measurement and annealing temperatures [32,49,50] indicates that centers, responsible for CL, have various natures. It means that the structure of the energy levels in the band gap of SnO_2 is complicated, and the presence in the band gap of SnO_2 of several trapping states should be taken into account. According to our assumptions, the energy diagram shown in Fig. 10 corresponds to those levels. We believe that inside of the SnO_2 band gap beside the shallow acceptor levels near the valence band that we have at the least three deep levels located at 0.8–0.9 eV, 1.3–1.4 eV, and ~1.6 eV from the top of the valence band.

While building this diagram, we supposed that the broad peaks of cathodoluminescence are a consequence of the participation of several close located levels during their formation. Moreover, due to the sufficient disorder (deviation from stoichiometry) of the SnO_2 structure, those levels can form zones with partial overlapping stimulating such strong broadening of the measured peaks. It is necessary to note that a large broadening of the CL spectra is a characteristic feature of materials with a natural deviation from stoichiometry. As it was established during our experiments, the annealing leads to the decrease of FWHM of the CL peaks that confirms our hypothesis of forming zones due to structural disorder.

The results of the excitation emission study, given in Ref. [35], are another confirmation of our model. In the spectra as presented in Ref. [35], the thin structure of the peak can be clearly seen, centered at 520 nm, confirming our conclusion about participation of several levels in broad peak forming. It turns out that the maximums of these peaks are shifted from each other along with the energy at 0.07–0.28 eV which is close to the difference in energy

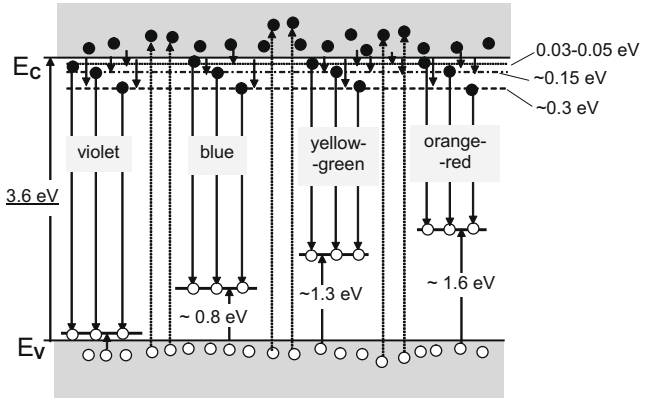

Fig. 10. Energetic scheme illustrating the position of levels in SnO_2 band gaps and transitions between these levels responsible for radiative recombination in SnO_2.

positions of shallow donor levels near the bottom of the conduction band. According to Refs. [4,5,30], in the band gap of SnO_2 there are several donor levels, located between 0.03–0.05 eV, ~0.13–0.15 eV, and ~0.3 eV from the bottom of the conduction band. The energy positions of those levels was determined on the basis of temperature dependencies of electron conductivity, thermally stimulated emission, and the data for electron spin resonance (ESR). Using the proposed energy diagram, it is possible to describe all of the observed spectra measured in the range of 350–800 nm for both un-doped and doped samples. The possibility of describing CL spectra of both the un-doped and doped samples using the same system of energy levels confirms the conclusion made before that doping with the elements that were used for this study, in spite of the strong influence on the concentration of individual defects, does not introduce additional defect centers of radiative recombination in the tested spectral range 300–800 nm. The centers with an energy position at 0.8–0.9 eV from the top of valence band are responsible for blue light emission ($\lambda \sim 440$–490 nm), the ones with energetic position at 1.3–1.4 eV from the valence band top are responsible for yellow–green light emission ($\lambda \sim 540$–580 nm), and the centers with an energetic position at ~1.6 eV from the top of valence band are responsible for orange–red light emission ($\lambda \sim 620$–690 nm). A similar approach was used earlier in Ref. [7] for an explanation of CL spectra of SnO_2 nanocrystalline powders and nanowires. However, that earlier study used an energy diagram containing only two levels at ~0.9 and 1.4 eV from the top of the valence band.

Analyzing the conclusions about the nature of the centers responsible for the appearance of different bands of luminescence it can be seen, as shown Table 2, that at present there is no reliable opinion about the nature of the centers which are responsible for radiative recombination in SnO_2. The structures associated with the charged defects in SnO_2 are not nearly as well described as for those in group IV and III–V semiconductors. The effects of variable charge states on defect configurations and relaxation has not often been explored in conjunction with tin dioxide. It means that for correct conclusions about the nature of the above-mentioned centers more deep and detailed studies in this area are still needed.

At the same time one can notice good correlation of suggested energy levels between 0.8–0.9 eV and 1.3–1.4 eV with values calculated in [7] by the *ab initio* method and ascribed to the energy levels of surface oxygen vacancy [50]. However, in opposition to the work of the authors of [7,50] considering the level, positioned at 0.9 eV over the valence band top as surface states, we believe that those centers, in spite of being in the surface area, are not the surface ones. Apparently they have a bulk nature (i.e. they are connected with the presence of bulk point defects). However, their concentration is maximal near the surface and decreases into the depth of the grain, which explains the increased role of those centers during the processes of radiative recombination in nano-dimensional powders and films where the structurally disordered area could extend over the whole grain's thickness. Our conclusion is confirmed by the need for long treatments at $T_{an} \sim 600$–650 °C up to 1–30 days for an attainment of a noticeable effect on photoluminescence spectra. As is already known, in order to create a considerable change in the concentration of oxygen vacancies at the SnO_2 surface, it is sufficient to do short-term treatment in the temperature range of 450–550 °C [2,3].

In [30] we have supposed that the peak centered at ~650–700 nm corresponds to radiative recombination with the participation of Sn interstitials ($E_V - E_t$ = ~1.6 eV). The results obtained during recent experiments have not changed our concepts about the nature of a present center. As it was established, the increase of the concentration of a doping impurity was accompanied by the increase of the role of the band peaked at $\lambda \sim 650$–700 nm in the CL spectra (see Fig. 6) which agrees with the suggested explanation of

Table 2
The nature of centers used for explanations of cathodoluminescence and photoluminescence spectra of SnO_2.

Peaks (nm)	Band-edge or shallow donor–acceptor pair transitions	Centers associated with oxygen vacancies	Centers associated with tin interstitial	Various structural defects	Oxygen vacancy-related surface states	Grain boundary
The nature of emission peaks						
300–360	[15,37]					
380–400	[12]	[17]	[37]	[6,16,18,33,52]	[50,51]	
420–450		[14]	[9,17]	[34]	[7]	[31]
480–520		[6,18,51]			[6,49]	[31]
540–560		[16]		[8,9]	[50,53]	
580–590		[51]	[30]		[7]	
640–650		[31]				

the nature of a present center. Moreover, as is already known, atoms of Co and Fe can occupy Sn's place in a SnO_2 lattice stimulating the formation of surplus concentrations of Sn interstitials [22]. Regarding the nature of other peaks, we do not have any productive ideas. The answer to this question requires additional research.

As for the effects of oxygen vacancies upon CL, according to our diagram it can be seen that the levels ascribed to oxygen vacancies manifest themselves in all processes of radiative recombination, that is all peaks observed in the CL spectra are related to O-vacancies. It means that the intensities of all the CL peaks should depend on both the concentration of oxygen vacancies and the concentration of structural defects as they affect the processes of both radiative and non-radiative recombination. This very fact determines the complicated character of the dependence of some CL peaks' intensities from deposition parameters following high temperature annealing [7,9,16,30,51]. In other words, for the attainment of the high CL intensity the SnO_2 should have optimal crystalline structure characterized by high crystallinity at high concentrations of oxygen vacancies which is quite a contradictory requirement.

4. Conclusion

It was found that SnO_2 films deposited by spray pyrolysis have CL spectra typical to synthesized SnO_2 powders and one-dimensional structures with maximums centered at $\lambda \sim 500$ nm. Thus, the increase of deposition temperatures and film thicknesses increases the CL intensity while the doping of Co, Cu, and Fe in the concentration range between 0 and 16 at.% strongly decreases the CL intensity.

Annealing in the range of 700–950 °C is accompanied by a strong increase of CL intensity and the change of the shape of CL spectra. The CL spectra acquire fine structure after high temperature annealing. However, the effects of annealing's influence on CL spectra depends on the film thickness and the dopant used. The intensive short-wavelength band peaked at 370 nm is close to the band-edge luminescence, and appeared only in the spectra of the films with thicknesses larger than 200–300 nm.

It was assumed that observed transformation of the CL spectra was a result of the change in the correlation between a well-crystallized core and a disordered surface layer in the SnO_2 grain conditioned by the change of both grain size and concentration of structural defects in the SnO_2 surface layer. In films deposited at low temperatures, in doped films, and in films with small grain sizes, the role of a disordered unstoichiometric surface layer in the forming CL spectra is dominant.

It was established that radiative recombination in SnO_2 films occurs through shallow donor levels associated with O-vacancies and trapped centers. It was also assumed that the CL spectra of SnO_2 in the spectral range 300–800 nm can be explained in the context of a model with three types of defects forming deep levels located at 0.8–0.9, 1.3–1.4, and ~1.6 eV from the top of the valence band. The concentration of those levels depends on the nature of the dopant used.

Acknowledgements

This work was supported by the Ministry of Science and Technology of the Korean Government, and by the Korean Science and Engineering Foundation (KOSEF) (Grant No. 2009-0078928). This research was partially supported by the World Class University (WCU) Program at the Gwangju Institute of Science and Technology (GIST) through a grant (Project No. R31-20008-000-10026-0) by the Ministry of Education, Science, and Technology (MEST) of Korea. Authors are also thankful to Dr. M. Zamoryanskaya and Prof. N.N. Syrbu for help in the measurement of CL and transmission spectra of the studied SnO_2 films.

References

[1] D.E. Williams, Semiconducting oxides as gas-sensitive resistors, Sens. Actuators B Chem. 57 (1999) 1–16.
[2] N. Barsan, M. Schweizer-Berberich, W. Gopel, Fundamental and practical aspects in the design of nanoscaled SnO_2 gas sensors: a status report, Frasenius J. Anal. Chem. 365 (1999) 287–304.
[3] M. Batzill, U. Diebold, The surface and materials science of tin oxide, Prog. Surf. Sci. 79 (2005) 47–154.
[4] S. Samson, C.G. Fonstad, Defect structure and electronic donor levels in stannic oxide crystals, J. Appl. Phys. 44 (1973) 4618–4621.
[5] Y. Mizokawa, S. Nakamura, ESR and electric conductance studies of the fine-powdered SnO_2, Jpn. J. Appl. Phys. 14 (1975) 779–804.
[6] S. Rani, S. Roy, C.N. Krar, M.C. Bhatnaga, Structure, microstructure and photoluminescence properties of Fe doped SnO_2 thin films, Sol. St. Commun. 141 (2007) 214–218.
[7] J.D. Prades, J. Arbiol, A. Cirera, J.R. Morante, M. Avella, L. Zanotti, E. Comini, G. Faglia, G. Sberveglieri, Defect study of SnO_2 nanostructures by cathodoluminescence analysis: Application to nanowires, Sens. Actuators B Chem. 126 (2007) 6–12.
[8] J.H. He, T.H. Wu, C.L. Hsin, K.M. Li, L.J. Chen, Y.K. Chueh, L.J. Chou, Z.L. Wang, Beaklike SnO_2 nanorods with strong photoluminescent and field-emission properties, Small 2 (2006) 116–120.
[9] S.S. Chang, S.O. Yoon, H.J. Parl, Characteristics of SnO_2 annealed in reducing atmospheres, Cer. Int. 31 (2005) 405–410.
[10] D.C. Halls, C. Leach, Spectroscopic cathodoluminescence studies of additive free zinc oxide and varistor ceramics, Acta. Mater. 46 (1998) 6237–6243.
[11] D. Calestani, L. Lazzarini, G. Salviati, M. Zha, Morphological, structural and optical study of quasi-1D SnO_2 nanowires and nanobelts, Cryst. Res. Technol. 40 (2005) 937–941.
[12] W.D. Yul, X.M. Li, X.D. Gao, Microstructure and photoluminescence properties of bulk-quantity SnO_2 nanowires coated with ZnO nanocrystals, Nanotechnology 16 (2005) 2770–2774.
[13] B. Wang, Y.H. Yang, C.X. Wang, G.W. Yang, Growth and photoluminescence of SnO_2 nanostructures synthesized by Au–Ag alloying catalyst assisted carbothermal evaporation, Chem. Phys. Lett. 407 (2005) 347–353.
[14] Y.C. Her, J.Y. Wu, Low-temperature growth and blue luminescence of SnO_2 nanoblades, Appl. Phys. Lett. 89 (2006) 043115.
[15] S.S. Pan, C. Ye, X.M. Teng, L. Li, G.H. Li, Localized exciton luminescence in nitrogen-incorporated SnO2 thin films, Appl. Phys. Lett. 89 (2006) 251911.
[16] J. Jeong, S.P. Choi, C.I. Chang, D.C. Shin, J.S. Park, B.T. Lee, H.J. Song, Photoluminescence properties of SnO_2 thin films grown by thermal CVD, Sol. St. Commun. 127 (2003) 595–597.
[17] F. Gu, M.K. Lu, X.F. Cheng, S.W. Liu, G.J. Zhou, D. Xu, D.R. Yuan, Luminescence of SnO_2 thin films prepared bu spin-coating method, J. Cryst. Growth 262 (2004) 182–185.

[18] J. Jeong, S.P. Choi, K.J. Hong, H.J. Song, J.S. Park, Structural and optical properties of SnO_2 thin films deposited by using CVD techniques, J. Korean Phys. Soc. 48 (2006) 960–963.
[19] G. Korotcenkov, Gas response control through structural and chemical modification of metal oxides: State of the art and approaches, Sens. Actuators B Chem. 107 (2005) 209–232.
[20] T. Fukumura, Y. Yamada, H. Toyosaki, T. Hasegawa, H. Kionuma, M. Kawasaki, Exploration of oxide-based diluted magnetic semiconductors toward transparent spintronics, Appl. Surf. Sci. 223 (2004) 62–67.
[21] H. Ohta, H. Hosono, Transparent oxide optoelectronics, MaterialsToday 7 (6) (2004) 42–51.
[22] M.R.C. Santos, P.R. Bueno, E. Longo, J.A. Varela, Effect of oxidizing and reducing atmosphere on the electrical properties of dense SnO_2 -based varistors, J. Eur. Cer. Soc. 21 (2001) 161–167.
[23] G. Korotcenkov, V. Brinzari, I. Boris, (Cu, Fe, Co or Ni)-doped SnO_2 films deposited by spray pyrolysis: Doping influence of film morphology, J. Mater. Sci. 43 (2008) 2761–2770.
[24] G. Korotcenkov, S.D. Han, (Cu, Fe, Co and Ni)-doped SnO_2 films deposited by spray pyrolysis: Doping influence on thermal stability of SnO_2 film structure, Mater. Chem. Phys. 113 (2009) 756–763.
[25] G. Korotcenkov, A. Cornet, E. Rossinyol, J. Arbiol, V. Brinzari, Y. Blinov, Faceting characterization of SnO_2 nanocrystals deposited by spray pyrolysis from $SnCl_4$-$5H_2O$ water solution, Thin Solid Films 471 (2005) 310–319.
[26] G. Korotcenkov, V. Brinzari, J. Schwank, A. Cerneavschi, Possibilities of aerosol technology for deposition of SnO_2 -based films with improved gas sensing characteristics, Mater. Sci. Eng. C 19 (2001) 73–77.
[27] G. Korotcenkov, V. Brinzari, M. DiBattista, J. Schwank, A. Vasiliev, Peculiarities of SnO_2 thin film deposition by spray pyrolysis for gas sensor application, Sens. Actuators B Chem. 77 (2001) 244–252.
[28] M.V. Zamoryanskaya, S.G. Konnikov, A.N. Zamoryanskaya, A high-sensitivity system for cathodoluminescent studies with the Camebax Electron Probe Microanalyzer, Instrum. Exp. Tech. 47 (2004) 477–483.
[29] G. Korotcenkov, V. Brinzari, M. Ivanov, A. Cerneavschi, J. Rodriguez, A. Cirera, A. Cornet, J. Morante, Structural stability of In_2O_3 films deposited by spray pyrolysis during thermal annealing, Thin Solid Films 479 (2005) 38–51.
[30] G. Korotcenkov, M. Nazarov, M.V. Zamoryanskaya, M. Ivanov, A. Cirera, K. Shimanoe, Cathodoluminescence study of SnO_2 powders aimed for gas sensor applications, Mater. Sci. Eng. B 130 (2006) 200–205.
[31] D. Maestre, A. Cremades, J. Piqueras, Cathodoluminescence of defects in sintered tin oxide, J. Appl. Phys. 95 (2004) 3027–3030.
[32] D. Maestre, R. Plugary, A. Cremades, J. Piqueras, Effect of thermal and mechanical treatments on the cathodoluminesce of tin and titanium oxides, Mater. Res. Soc. Symp. 738 (2003) G.2.4.1–G.2.4.6.
[33] H.W. Kim, N.H. Kim, J.H. Myung, S.H. Shim, Characteristics of SnO_2 fishbone-like nanostructures prepared by the thermal evaporation, Phys. Stat. Sol. (a) 202 (2005) 1758–1762.
[34] J.Q. Hu, X.L. Ma, N.G. Shang, Z.Y. Xie, N.B. Wong, C.S. Lee, S.T. Lee, Large-scale rapid oxidation synthesis of SnO_2 nanoribbons, J. Phys. Chem. B 106 (2002) 3823–3826.
[35] B. Yu, C. Zhu, F. Gan, Exaction spectra of SnO_2 nanocrystals with surficial dipole layer, Opt. Mater. 7 (1997) 15–20.
[36] X. Wu, B. Zou, J. Xu, B. Yu, G. Tang, G. Zhang, W. Chen, Structural characterization and optical properties of nanometer-sized SnO_2 capped by stearic acid, Nanostruct. Mater. 8 (1997) 179–189.
[37] F. Gu, S.F. Wang, C.F. Song, M.K. Lu, Y.X. Qi, G.J. Zhou, D. Xu, D.R. Yuan, Synthesis and luminescence properties of SnO_2 nanoparticles, Chem. Phys. Lett. 372 (2003) 451–454.
[38] G. Korotcenkov, M. Nazarov, M.V. Zamoryanskaya, M. Ivanov, Cathodoluminescence emission study of nanocrystalline In_2O_3 films deposited by spray pyrolysis, Thin Solid Films 515 (2007) 8065–8071.
[39] J. Kang, S. Tsunekawa, A. Kasuya, Ultraviolet absorption spectra of amphoteric SnO_2 nanocrystallites, Appl. Surf. Sci. 174 (2001) 306–309.
[40] J.X. Zhou, M.S. Zhang, J.M. Hong, X. Yin, Raman spectroscopic and photoluminescence study of single-crystalline SnO_2 nanowires, Sol. St. Commun. 138 (2006) 242–246.
[41] A. Cabot, J. Arbiol, J.R. Morante, U. Weimar, N. Barsan, W. Gopel, Analysis of the noble metal catalytic additives introduced by impregnation of as obtained SnO_2 sol–gel nanocrystals for gas sensors, Sens. Actuators B Chem. 70 (2000) 87–100.
[42] A. Cabot, A. Dieguez, A. Romano-Rodriguez, J.R. Morante, N. Barsan, Influence of the catalytic introduction procedure on the nano-SnO_2 gas sensor performances. Where and how stay the catalytic atoms?, Sens Actuators B Chem. 79 (2001) 98–106.
[43] S. Gutzov, M. Bredol, F. Wasgestian, Cathodoluminescence study of europium-doped zirconia and cassiterite powders, J. Phys. Chem. Sol. 59 (1998) 69–74.
[44] N. Maneva, K. Kynev, L. Grigorov, L. Lijutov, Luminescence efficiency of SnO_2: Eu and rate of SnO oxidation, J. Mater. Sci. Lett. 16 (1997) 1037–1039.
[45] C. Nayral, E. Viala, V. Colliere, P. Fau, F. Senocq, A. Maisonnat, B. Chaudret, Synthesis and use of a novel SnO_2 nanomaterial for gas sensing, Appl. Surf. Sci. 164 (2000) 219–226.
[46] A. Dieguez, A. Romano-Rodriguez, A. Vila, J.R. Morante, The complete Raman spectrum of nanometric SnO_2 particles, J. Appl. Phys. 90 (2001) 1550–1556.
[47] S. Wen, D. Yan, Grain boundary in some nano-materials, Cer. Intern. 21 (1995) 109–112.
[48] A. Cirera, A. Cornet, J.R. Morante, S.M. Olaizola, E. Castano, J. Gracia, Comparative structural study between sputtered and liquid pyrolyisis nanocrystalline SnO_2, Mater. Sci. Eng. B 69–70 (2000) 406–410.
[49] S. Luo, J. Fan, W. Liu, M. Zhang, Z. Song, C. Lin, X. Wu, P.K. Chu, Synthesis and low-temperature photoluminescence properties of SnO_2 nanowires and nanobelts, Nanotechnology 17 (2006) 1695–1699.
[50] X.T. Zhou, F. Heigl, M.W. Murphy, T.K. Sham, T. Regier, I. Coulthard, R.I.R. Blyth, Time-resolved X-ray excited optical luminescence from SnO_2 nanoribbons: Direct evidence for the origin of the blue luminescence and the role of surface states, Appl. Phys. Lett. 89 (2006) 213109. 3p.
[51] S. Luo, P. Chu, Origin of low-temperature photoluminescence from SnO_2 nanowires fabricated by thermal evaporation and annealing in different ambient, Appl. Phys. Lett. 88 (2006) 183112. 3p.
[52] L. Huang, L. Pu, Y. Shi, R. Zhang, B. Gu, Y. Du, Controlled growth of well-faceted zigzag tin oxide mesostructures, Appl. Phys. Lett. 87 (2005) 163124. 3p..
[53] S.S. Chang, D.K. Park, Novel Sn powder preparation by spark processing and luminescence Properties, Mater. Sci. Eng. B 95 (2002) 55–60.